Kinetic modeling of *in vitro* small intestinal lipid digestion as affected by the emulsion interfacial composition and gastric pre-lipolysis

Marcos R. INFANTES-GARCIA[*], Sarah H.E. VERKEMPINCK, Marc E. HENDRICKX, Tara GRAUWET[**]

Laboratory of Food Technology, Leuven Food Science and Nutrition Research Centre (LFoRCe), Department of Microbial and Molecular Systems (M^2S), KU Leuven, Kasteelpark Arenberg 22, PB 2457, 3001 Leuven, Belgium.

Journal: Journal of Agricultural and Food Chemistry

Submitted: January 2021

Re-submitted: March 2021

[*]author whom correspondence should be addressed during submission process:

marcos.infantes@kuleuven.be

+32 16 37 65 53

[**] author whom correspondence should be addressed post-publication:

tara.grauwet@kuleuven.be

+32 16 32 19 47

Abstract

This research evaluated the impact of the emulsion interfacial composition on *in vitro* small intestinal lipolysis kinetics with the inclusion of rabbit gastric lipase resulting in a gastric pre-lipolysis step. O/w emulsions contained 5% triolein (w/w) and 1% (w/w) of the following emulsifiers: sodium taurodeoxycholate, citrus pectin, soy protein isolate, soy lecithin and tween 80. Emulsions were subjected to static *in vitro* digestion and diverse lipolysis species quantified via HPLC-charged aerosol detector. Single-response modeling indicated that kinetics of lipolysis in the small intestinal phase were impacted by the emulsion particle size at the beginning of this phase. Multi-response modeling permitted the elucidation of the lipolysis mechanism under *in vitro* conditions. The final reaction scheme included enzymatic and chemical conversions. The modeling strategies used in this research allowed to gain more insight on the kinetics and mechanism of *in vitro* lipid digestion.

Keywords

Emulsion interfacial composition; lipid digestion; *in vitro*; kinetic modeling; gastric lipase; pancreatic lipase

Introduction

The digestion of lipids in oil-in-water (o/w) emulsions is a phenomenon that depends on the extent of lipase adsorption at the oil-water interface [1,2]. Consequently, the composition of the emulsion interface influences phenomena directly related to lipid digestion: (*i*) the interfacial displacement of the emulsifier by bile salts and lipases; (*ii*) the emulsion stability under digestive conditions; (*iii*) the potential hydrolysis of emulsifiers at the interface, and *(iv)* the micellization and transport of lipolysis products. The competitive adsorption between lipase, bile salts and emulsifiers at the interface refers to the capacity of the former ones to displace the original emulsifier so the lipid digestion process can proceed [3,4]. Recently, it has been shown that dog gastric lipase adsorption was blocked by using adsorbed polymer particles in an o/w emulsion [5]. Next to this, the physicochemical properties of the emulsifier(s) used can largely influence the emulsion stability under digestion conditions. As a consequence, the available surface area for lipase adsorption can be significantly modified causing changes in the kinetics of lipid digestion [6–9]. Another implication of the interfacial composition is the potential hydrolysis of emulsifiers present at the interface (e.g. protein- or digestible carbohydrate- or lipid-based stabilizers) [10]. This phenomenon can influence emulsion stability as well as the interaction between these hydrolyzed surface-active compounds and digestive elements (i.e. lipases and bile salts). Micellization and transport of lipolysis products could also be supported by emulsifiers with micellization capacity if these are present in the initial emulsions (e.g. phospholipids).

The engineering of emulsion properties from a digestibility perspective could have diverse applications, e.g. to increase lipophilic bioactives bioavailability or to affect satiety [11,12]. Vast research has been conducted to evaluate this effect under simulated small intestinal conditions [13–18]. Nonetheless, only a limited amount of *in vitro* studies have included a relevant substitute of

human gastric lipase to evaluate the impact of gastric pre-lipolysis on the subsequent small intestinal phase [16,19,20]. Moreover, quantification of diverse lipolysis species, monitoring of emulsion stability during *in vitro* digestion, and/or use of emulsifiers of different chemical nature is still lacking in the state-of-the-art research.

The study of reaction kinetics taking place in food systems implies the application of suitable quantification techniques to collect relevant data, and appropriate mathematical modeling methods to quantitatively compare kinetic parameters [21]. When evaluating the effect of emulsion properties on lipid digestion kinetics, few studies have attempted to apply modeling techniques to understand this phenomenon [15,18,22–24]. Most research in this field have evaluated results from different treatments/conditions by visual comparison or basic statistical analysis (ANOVA and *post hoc* comparison tests). In addition, a common feature in most recent studies assessing the lipolysis kinetics as affected by emulsion design properties is the quantification of FFA release via titration as a sole response [25]. Drawbacks of this technique are the lack of information about enzymatic conversions of intermediate products, low sensitivity and report of odd results (e.g. FFA release extents higher than 100%). The quantification of multiple lipid digestion species could allow to overcome these flaws and moreover give mechanistic insight on the lipolysis reactions. Some fundamental studies in which the stereoselectivity of lipases was analyzed have employed chromatographic techniques to quantify the release of multiple lipid digestion products (e.g. tri, di-, monoglycerides, and fatty acids) [26–28]. However, to the best of our knowledge, limited information can be found regarding the quantification of multiple lipolysis species (including isomers) when studying the effect of emulsion design properties on *in vitro* lipid digestion.

In this research, our objective was (*i*) to assess the effect of the emulsion interfacial composition on the kinetics of small intestinal lipid digestion after a gastric pre-lipolysis step by means of

single-response modeling and relating it to the emulsion stability during the gastric phase, and (*ii*) to elucidate the lipolysis molecular mechanism under static *in vitro* small intestinal conditions in presence of gastric and pancreatic lipases by using the advanced multi-response modeling technique. To achieve these objectives, emulsions were prepared with triolein (5%) and a stabilizing agent (1%) which selection was based on a diverse stability performance and chemical nature: sodium taurodeoxycholate (NaTDC), lecithin (LEC), soy protein isolate (SPI), citrus pectin (CP) or tween 80 (TW80). NaTDC is a purified bile salt, which can be potentially employed in self-emulsifying systems [29]. LEC is an ionic stabilizing agent commonly used in food formulations. TW80 is an edible non-ionic surfactant, stable over a broad pH range. SPI is an ionic food polymer, employed as stabilizer in meat products, cake batters, coffee whiteners, milks, mayonnaise, salad dressings, and frozen desserts [30]. CP is a indigestible carbohydrate, found in the waste streams of the citrus industry. CP has shown a good emulsifying and stabilizing capacity in model emulsions [31]. The substrate for lipases was triolein. We selected this purified oil because it is abundant in commercial oils like olive, canola and high oleic sunflower oil [32]. Moreover, triolein hydrolysis can generate isomers that can be further quantified to obtain mechanistic insight on lipid digestion reactions.

Materials and methods

Preparation of emulsions

Different emulsifying agents were individually employed to prepare a series of emulsions: sodium taurodeoxycholate (> 95%, Cayman Chemical Company, MI, USA), lecithin (98% phosphatidylcholine, PanReac AppliChem, Darmstadt, Germany), soy protein isolate (90%, Bulk Powders, Colchester, UK), citrus pectin (degree of methylesterification ≥ 85%, Sigma-Aldrich,

Diegem, Belgium) or tween 80 (Sigma-Aldrich, Diegem, Belgium). Emulsions contained triolein (5% w/w) (> 99%, Acros Organics, Geel, Belgium), one type of the above mentioned emulsifying agents (1% w/w) and Milli-Q water (94% w/w). First, coarse emulsions were prepared using a high-shear mixer (Ultra-Turrax T25, IKA, Staufen, Germany) at 13500 rpm for 5 min. For CP and SPI, these compounds were first dissolved or dispersed in water overnight under constant stirring prior to mixing with the oil. Second, the coarse emulsions were subjected to one cycle of homogenization at 100 MPa in a high-pressure homogenizer (Stansted SPCH-10, Homogenizing systems, U.K.) to form a fine emulsion [33].

In vitro digestion of the generated emulsions

In this study, a kinetic approach was followed to analyze the time dependent evolution of *in vitro* digestion. Hence, one independent, end-point moment for the gastric phase (i.e. 120 min after addition of gastric enzymes) and eight independent moments for the small intestinal phase (i.e. 5; 10; 15; 30; 45; 60; 90; 120 min after addition of pancreatic enzymes enzymes) were considered to evaluate the digestion kinetics per emulsion type. For this purpose, we utilized the standardized protocol of the international network INFOGEST [34]. In this method, static conditions are used for each digestion compartment, which means that physiological parameters are set at the beginning of each digestion phase. We down-scaled the *in vitro* digestion experiment to reduce the consumption of chemical products and enzymes as explained in our previous work [33].

Gastric phase. In a brown vial (to avoid oxidation of lipids), volumes of 125 µL of emulsion and 125 µL of Milli-Q water were mixed to simulate dilution by saliva in the oral phase. In a next step, we added 200 µL of simulated gastric fluid set at pH 3, and 5 µL of a 15 mM $CaCl_2$ solution. Afterwards, 15 µL of a rabbit gastric extract (RGE, Lipolytech Marseille, France) solution, containing pepsin and rabbit gastric lipase, was added to mimic gastric lipid digestion (RGE was

dissolved in Milli-Q water). RGE lipase activity was experimentally measured (19.9 ± 1.3 U/mg tributyrin-based). Then, HCl 50 mM was added to reach a pH value of 3. The exact HCl volume was determined in a preliminary up-scaled experiment and was different for each emulsion. Lastly, enough Milli-Q water was added to reach a final chyme volume of 0.5 mL. In each digestion vial, a gastric lipase activity of 60 U/mL (tributyrin-based) and consequently a pepsin activity of 2340 U/mL (hemoglobin-based) was reached. The above mentioned volumes were added to all eight independent samples intended for studying the small intestinal phase kinetics. For end-point gastric phase samples per emulsifier type, the double of these aliquots were added to reach a final volume of 1 mL. Each vial headspace was filled with nitrogen, whereafter the vials were incubated at 37 °C. The stomach mechanical agitation was mimicked with an end-over-end rotator set at 40 rpm. Gastric lipid digestion reactions were stopped via chemical inhibition. In case of the end-point gastric phase sample, we added 10 µL of a 100 mM Orlistat (Sigma-Aldrich, Diegem, Belgium) ethanol solution to inhibit lipid digestion. The remaining eight independent tubes per emulsifier type were further processed in the small intestinal phase without gastric lipase inhibition.

Small intestinal phase. The brown vials from the gastric phase were opened and a series of solutions were added to the 0.5 mL of chyme. First, 200 µL of simulated intestinal fluid set at pH 7, and 40 µL of a 15 mM $CaCl_2$ solution were incorporated. Subsequently, we added 75 µL of bile salts solution (to reach 10 mM in the chyle). Bile salts content in the bile extract (Sigma-Aldrich, Diegem, Belgium) was determined (1.24 mmol/g powder). Then, an aliquot of 125 µL of pancreatin was added to reach 2000 U/mL of lipase activity using tributyrin as substrate. Pancreatic extract powder was kindly donated by Nordmark (Uetersen, Germany), and presented an experimentally determined lipase activity of 125 U/mg (tributyrin-based). Finally, NaOH (50 mM) was included in the reaction mixture to reach a pH value of 7 (the exact volume was determined

in a preliminary up-scaled experiment, and depended on the emulsifier used). The total chyme volume was 1 mL after adding enough Milli-Q water. The headspace of each vial was again filled with nitrogen, incubated at 37 °C, and agitated with an end-over-end rotator set at 40 rpm. Lipolysis in the small intestinal phase was stopped by adding 10 µL of 100 mM Orlistat and 10 µL of an 4-bromophenylboronic acid (Sigma-Aldrich, Diegem, Belgium) solution (1 M in methanol) to inhibit gastric lipase and pancreatic lipase, respectively. All samples were kept on ice until lipid extraction was started immediately after the digestion experiment was finished.

Oil droplet physicochemical properties

The particle charge, microstructure, and particle size were determined in the emulsions and their respective digested samples taken at different digestion moments (after 120 min of gastric phase; and 15, 30, 60 and 120 min of intestinal phase). These oil droplet properties are indicators for the emulsion stability evolution during *in vitro* digestion [24,33].

Particle charge

The oil droplet ζ-potential in the initial emulsion and digested samples was determined via dynamic light scattering electrophoresis equipment (Zetasizer NanoZS, Malvern Instruments, Worcestershire, UK). Emulsion, gastric, and small intestinal phase samples were diluted (1:10) with pure Milli-Q water, Milli-Q water adjusted to pH 3, or to pH 7, respectively before analysis. We performed these measurements in duplicate per sample type [33].

Microstructure

We observed the microstructure of the initial emulsions (1:4 dilution with Milli-Q water) and their respective digested samples (no dilution) using an optical microscope (Olympus BX-41) equipped

with an Olympus XC-50 digital camera (Olympus, Opticel Co. Ltd., Tokyo, Japan). Samples microstructure was observed at 40x magnification [33].

Particle size

Initial emulsions and digested samples were also analyzed in a laser diffraction equipment (Beckman Coulter Inc., LS 13 320, FL, USA). We determined the particle size distribution and volume-weighted mean particle size d(4,3) in duplicate applying the same settings as described in our previous work [33].

Quantification of lipid digestion products

From triolein (TAG) hydrolysis, diverse hydrolysis products can be generated: *sn*-1,2/2,3-diolein (*sn*-1,2/2,3-DAG); *sn*-1,3-diolein (*sn*-1,3-DAG); *sn*-2-monoolein (*sn*-2-MAG); *sn*-1/3-monoolein (*sn*-1/3-MAG) and oleic acid (FFA). All these neutral lipids were immediately extracted after performing the digestion experiment and stored at -80 °C for maximally one week. Lipid extraction and HPLC-CAD quantification were exactly carried out following the procedure indicated in our previous work [33]. The concentration of glycerol (GLY) per digestion moment was calculated by performing a molar balance of the lipolysis products as explained in the previously cited study.

Statistical analysis and modeling

One-way ANOVA and comparison test

We statistically compared the changes in volume-weighted mean droplet size and ζ-potential during *in vitro* digestion. Therefore, we utilized the software JMP (JMP pro14, SAS Institute Inc., Cary, NC, USA) to carry out an one-way ANOVA and Tukey HSD comparison tests to determine significant differences ($P < 0.05$) among samples during *in vitro* digestion.

Single-response kinetic modeling

Lipolysis kinetics during the small intestinal phase were evaluated via single-response modeling using the software JMP (JMP pro14, SAS Institute Inc., Cary, NC, USA). For this type of modeling, we selected the ratio of TAGs digested during the small intestinal phase over the initial TAGs concentration in the emulsion as a response. We employed an empirical, fractional conversion model to compare the kinetic parameters of the different emulsions under *in vitro* small conditions [35]. This technique allowed the estimation of kinetic parameters which are specified in equation (1). The term C (%) represents the predicted response at time t (min) during the small intestinal phase. The estimated parameters are: the asymptotic value C_f (%); the initial value C_0 (%) (t=0); and the reaction rate constant k (min^{-1}).

$$C = C_f + (C_0 - C_f)e^{-kt} \quad (1)$$

We compared the estimated kinetic parameters (C_0, C_f and k) by calculating their confidence intervals (95%).

Multi-response kinetic modeling

We aimed to obtain mechanistic insight into the lipolysis reaction in the small intestinal phase by means of multi-response modeling. This advanced modeling technique has been previously utilized in our research unit. A reaction scheme of lipolysis in the small intestinal phase in presence of lipases from a pancreatic extract was proposed [23]. Recently, our research group postulated a mechanism of gastric lipolysis in presence of gastric lipase which consisted of both enzymatic and chemical conversions [24,33]. In the present study, we aimed to understand the lipid digestion mechanism in the small intestinal phase in presence of gastric as well as pancreatic lipases.

193 The first step of multi-response modeling was to propose a reaction scheme based on the available
194 literature regarding the lipid digestion mechanism and the data generated in this study. Afterwards,
195 the proposed (bio)chemical reactions were transformed into differential equations. These equations
196 contained the concentrations of diverse lipolysis products quantified by HPLC-CAD, and reaction
197 rate constants (k, min^{-1}) that were estimated with this advanced methodology. We estimated the
198 kinetic parameters by solving the differential equations with the 'proc model' command of the
199 statistical software SAS (version 9.4, SAS Institute Inc., Cary, NC, USA). A variable order,
200 variable step-size backward difference scheme was employed to integrate the differential
201 equations. We employed the full information maximum likelihood (FIML) and the Gauss-Newton
202 minimization methods to estimate the kinetic parameters. The concentrations of *sn*-1,2/2,3-DAG;
203 *sn*-1,3-DAG; *sn*-2-MAG; *sn*-1/3-MAG; FFA and GLY at the starting point of intestinal digestion
204 were set equal to the experimentally determined concentrations at the end of the gastric phase. We
205 made use of the 'fit' statement with standard options and set the 'dynamic' option as well as a
206 convergence criterion of 0.01, and the maximum number of iterations equal to 500 [23,24,33].

207 # Results and discussion

208 ## Changes in oil droplet properties during *in vitro* digestion

209 Some indicators of emulsion stability were followed during *in vitro* digestion because these
210 properties may drastically influence lipolysis kinetics. The oil droplet charge can give information
211 about interfacial electrostatic interactions impacting the overall emulsion stability. Emulsion
212 microstructure and particle size give complementary indication of emulsion (in)stability (e.g.
213 coalescence or flocculation). The volume-based average particle size d(4,3) of the different initial

emulsions was initially equivalent: 0.94 ± 0.00 μm for NaTDC-, 1.31 ± 0.04 μm for LEC-, 1.10 ± 0.05 μm for SPI-, 1.12 ± 0.16 μm for CP-, and 0.78 ± 0.03 μm for TW80-based emulsions.

NaTDC emulsion. The oil droplet characteristics presented a variable trend during digestion. The ζ-potential of the initial emulsion was largely negative due to the ionic nature of the emulsifier (-79.9 mV at pH 6.8). Yet, after 2 hours of gastric digestion, the droplet charge changed to a slightly positive value (Figure 1). As observed in Figure 2 and the Supp. information, simulated gastric conditions drastically increased the particle size of the emulsion indicating a large extent of emulsion droplet coalescence. Therefore, the ζ-potential measured at the end of the gastric phase probably represents the ions solubilized in the aqueous phase as the emulsion showed phase separation. The reason for this phenomenon may be the formation of micelles between NaTDC molecules and lipid digestion products causing a removal of NaTDC molecules from the interface. This probably led to the destabilization of oil droplets resulting in a high extent of emulsion coalescence (Figure 2 and Supp. Information). A different scenario occurred during the small intestinal phase. The ζ-potential after 15 min of small intestinal digestion became negative because of bile salts and phospholipids adsorption to the interface added in the bile extract. During this phase, Figure 1 depicts a gradual decrease in the droplet charge which may represent the formation of free fatty acids and/or micellar structures [35]. In case of the particle size, we observed a progressive decrease which can be due to a structuring effect by the addition of bile salts. The role of bile salts in emulsification of lipids during digestion is widely acknowledged [36,37]. This structuring phenomena could also be promoted by lipolysis products with surface active properties (e.g. monoglycerides).

LEC emulsion. The ζ-potential was considerably negative because the phospholipids were ionized at the pH of the emulsion (8.0). At the end of the gastric phase, the droplet charge changed to 5.8

237 mV. This charge sign change possibly occurred due to the adsorption of positive ions added with
238 the simulated fluids onto the negatively charged phosphates groups of the emulsifier resulting in a
239 shielding effect [38,39]. The positive droplet charge could also be influenced by the pH decrease
240 during the gastric phase (from 8 to 3), which changed the charge of the phospholipids. The particle
241 size slightly increased during this phase, mainly due to coalescence (Figure 2 and Supp.
242 Information). The generation of lipolysis products during this phase possibly also contributed to
243 the stabilization of oil droplets. Along the small intestinal phase, the ζ-potential evolution had an
244 analogous behavior as the NaTDC-based emulsion due to fatty acids production and micelles
245 formation. The particle size rapidly augmented during the first 30 min of small intestinal digestion
246 due to flocculation. Afterwards, lipid digestion caused the gradual disappearance of oil droplets
247 leading to a particle size decrease observed until the end of this phase. A comparable behavior was
248 observed for a lysolecithin-stabilized emulsion during *in vitro* small intestinal phase [13].

249 **SPI emulsion.** It presented a negative droplet charge due to the pH value of the emulsion (8.0)
250 which is above the isoelectric point of soy proteins [40] (Figure 1). During the gastric phase, the ζ-
251 potential shifted towards a positive value due to the acid pH (lower than isoelectric point of soy
252 proteins). Afterwards, it gradually became more negative possibly due to the release of free fatty
253 acids and/or the hydrolysis of adsorbed soy proteins. Protein digestion has shown to decrease the
254 net surface charge of protein-stabilized emulsions [41]. About the particle size, it moderately
255 increased until an average value of 10 μm after 120 min of gastric digestion mainly due to
256 flocculation (Figure 2 and Supp. information). Even if protein stabilizing the oil droplets were
257 partially cleaved by pepsin potentially causing emulsion instability, generated peptides and
258 lipolysis products can stabilize oil droplets as previously reported [41,42]. In case of the small
259 intestinal phase, bile salt adsorption, formation of fatty acids and proteolysis turned the ζ-potential

into negative values which became more negative over digestion time. The mean particle size of the SPI-stabilized emulsion drastically increased after 15 min of small intestinal digestion. Then, it decreased to values between 12-27 μm during the remaining small intestinal phase. A structuring phenomena occurring in this case can possibly be linked to the formation of micelles and production of lipolysis products resulting in smaller oil droplets.

CP emulsion. This emulsion exhibited a droplet electrical charge of -20.1 mV (Figure 1). During gastric digestion, the acid pH changed the ζ-potential magnitude to a slightly positive magnitude because it was close to pectin pKa, while the particle size increased to a value of 18 μm due to a combined effect of flocculation and coalescence (Figure 2 and Supp. information). Similar results were encountered for CP-based emulsions of different methyl esterification degrees subjected to *in vitro* gastric digestion in absence of gastric lipase [43,44]. In case of the small intestinal phase, the ζ-potential followed a similar trend compared to the previous emulsions. The particle size augmented to values around 32-35 μm due to flocculation as observed in Figure 2. Similar findings were encountered for the same type of CP in a previous work [43].

TW80 emulsion. As observed in Figure 1, the initial ζ-potential value was -1.4 mV. This almost neutral charge was expected since TW80 is a non-ionic surfactant. The slightly negative charge may be caused by some free fatty acid impurities present in the emulsifier or the adsorption of OH^- groups at the oil-water interface [17]. During gastric digestion, the ζ-potential and mean particle size magnitude did not significantly change. However, during the small intestinal phase, an increase in the d(4,3) value was detected after 15 min of digestion due to flocculation (Figure 2). Hereafter, there was a progressive decrease in the magnitude of this property because oil droplets disappeared due to lipid digestion and formation of micelles. Regarding the ζ-potential, again negative values were observed during small intestinal digestion due to bile salts adsorption, fatty acid release and

micelles formation. This behavior in ζ-potential was also described for a tween-20-stabilized emulsion [13].

Lipid digestion products formation during small intestinal *in vitro* digestion

The analytical platform utilized in this work permitted the identification and quantification of the substrate triolein (TAG) and its corresponding lipolysis products: *sn*-1,2/2,3-diolein (*sn*-1,2/2,3-DAG); *sn*-1,3-diolein (*sn*-1,3-DAG); *sn*-2-monoolein (*sn*-2-MAG); *sn*-1/3-monoolein (*sn*-1/3-MAG) and oleic acid (FFA) (Figure 3). The product glycerol (GLY) was calculated based on the excess of FFA per digestion time (Section 2.5.2). As indicated in our previous work, the analytes *sn*-1,2/2,3-DAG and *sn*-1/3-monoolein represent the optical isomers of *sn*-1,2 and *sn*-2,3-DAG, and *sn*-1 and *sn*-3 MAG, respectively [24,33]. As observed in Figure 3, the initial values of triolein are different and the ones of the derived lipolysis products are not equal to zero (*t*=0 min, end of gastric phase). This is because gastric lipase acted on triolein to generate intermediate and final products during the gastric phase. In case of residual TAG and released FFA, concentrations at the end of the gastric phase were 24 and 5 μmol/mL for the NaTDC emulsion; 10 and 29 μmol/mL for the CP emulsion; 11 and 31 μmol/mL for the SPI emulsion; 14 and 18 μmol/mL for the LEC emulsion; and 27 and 1 μmol/mL for the TW80 emulsion, respectively. These initial values found in the present study are very close to the ones quantified in our previous, independent study, in which kinetics of gastric lipolysis as influenced by the emulsion interfacial composition were investigated [33].

Overall, during the small intestinal phase, a very fast hydrolysis of triolein occurred which resulted in the generation of intermediate and final products. The two regioisomers of diolein were produced in a low extent during the first 5-30 min of small intestinal digestion and then hydrolyzed. As depicted in Figure 3B-E, MAGs were produced in a higher extent compared to DAGs. The

306 intermediate products *sn*-1,2/2,3-DAG and particularly *sn*-2-monoolein were produced more
307 extensively compared to their corresponding regioisomers *sn*-1,3-DAG and *sn*-1/3-MAG,
308 respectively. This finding is logic since pancreatic lipase was the main enzyme active at the pH of
309 the small intestinal phase. This enzyme is regioselective for the *sn*-1 and 3 positions of the glycerol
310 moiety, which results in the predominant formation of *sn*-2-monoolein [45]. Yet, the detection of *sn*-
311 1,3-DAG and *sn*-1/3-MAG may be an indicator of certain yet lower activity over the *sn*-2 position.
312 We hypothesize that gastric lipase was still active during the small intestinal phase and responsible
313 for *sn*-2 position hydrolysis. It was reported that gastric lipase contribution to small intestinal
314 lipolysis was around 7.5% in an clinical trial [46]. In our previous studies, we obtained more
315 mechanistic insight in the gastric lipolysis reactions [24,33]. One interesting finding was the
316 establishment of a reaction scheme in which *sn*-2 position cleavage by gastric lipase was included.
317 Other authors also reported gastric lipase activity over the *sn*-2 position through the detection of
318 diolein enantiomers but did not propose a reaction mechanism based on other lipolysis products
319 [47,48].

320 In Figure 3A-G, we can also observe a significant effect of the initial emulsion interfacial
321 composition on the evolution of lipolysis products during small intestinal digestion. In case of
322 NaTDC-based emulsion, its instability during the gastric phase and further structuring by bile salts
323 during the small intestinal phase played an important role during lipid digestion. Triolein
324 hydrolysis and the formation of lipolysis products were delayed in comparison to the other
325 emulsions due to the large average particle size present in the first 60 min of small intestinal
326 digestion (Figure 2). A remarkable finding in Figure 3F-G is the significant lower extent of final
327 products generation for the NaTDC-based emulsion during the small intestinal phase. This can be
328 related to the lower hydrolysis degree of intermediate products (DAG and MAG) leading to a

329 lower formation of final products (FFA and GLY) due to emulsion coalescence as a result of
330 emulsion gastric instability. The instability phenomenon occurring during the gastric phase
331 explained in Section 3.1 drastically reduced the surface area available for lipase adsorption during
332 the first term of the small intestinal phase.

333 For all other emulsions, triolein was almost completely hydrolyzed within the first 15 min of small
334 intestinal digestion (Figure 3A). As observed in Figure 3B-E, there were some differences in the
335 trends of intermediate products formation and hydrolysis. LEC- and CP-based emulsions showed
336 a lower extent of intermediate products evolution compared to SPI- and TW80-based emulsions,
337 specially the monoolein regioisomers. This means that the intermediate products of LEC- and CP-
338 based emulsions were converted faster to final products. This observation is evidenced in Figure
339 3G, where glycerol formation extent is higher for LEC- and CP-based emulsions. In case of the
340 SPI-based emulsion, the slower hydrolysis of intermediate products may have occurred due to the
341 drastic increase in d(4,3) during the first minutes of small intestinal digestion (Figure 2). This
342 instability phenomena may hinder the removal of lipolysis products from the interface by bile salts
343 and subsequently lipase adsorption, thus causing accumulation of these intermediate products at
344 the droplet interface [49]. For the TW80-based emulsions, the limited TAG hydrolysis during the
345 gastric phase implied that the cleavage of TAGs predominantly occurred during the small intestinal
346 phase, so the intermediate products were produced later compared to the CP- and LEC-based
347 emulsions. This means that gastric pre-lipolysis influenced the formation and degradation of
348 intermediate products in the small intestinal phase. Other researchers also found that a LEC-
349 stabilized emulsion was more extensively digested under *in vitro* small intestinal conditions with
350 a gastric lipolysis step than sodium-caseinate- and tween-80-stabilized emulsions [16].

In order to evaluate the effect of gastric lipolysis on the following small intestinal lipolysis, it may be relevant to compare our results with other studies employing a similar experimental setup, specifically the same gastrointestinal conditions (i.e. INFOGEST protocol) without the inclusion of gastric lipase. In case of the FFA generation during small intestinal digestion, previous studies found that a TW80-based emulsion reached the highest and fastest production of this analyte during *in vitro* small intestinal digestion compared to other emulsions [13,43]. These observations are aligned with our results presented in Figure 3F, in which the TW80-based emulsion reached a high extent of FFA production. If we compare the evolution of FFA in the study of Verkempinck et al. and ours for the TW80 emulsion (Figure 3F), they look rather similar. In the same article by Verkempinck et al., citrus pectin with the same chemical characteristics to the one employed in our study was used to stabilize an emulsion subjected to *in vitro* digestion. In terms of emulsion stability, both emulsions showed a similar behavior during the whole *in vitro* digestion process. In our study, the CP-based emulsion exhibited a comparable FFA production trend in the small intestinal phase with respect to the TW80-based emulsion. However, the extent of FFA production in the small intestinal phase reported by Verkempinck et al. was much lower (<50%) compared to the TW80 emulsion. The difference between the results of Verkempinck et al. and ours might be explained by the gastric pre-lipolysis step which had a high contribution of FFA generated during the gastric phase. In other words, gastric lipolysis seemed to significantly affect the production of FFA in the to the small intestinal phase in case of the CP-based emulsion.

Our study includes the identification and quantification of diverse lipid digestion products which are part of simultaneous and consecutive lipase-catalyzed reactions. Therefore, we aimed to evaluate this data using two modeling strategies. A first strategy considers the selection of one representative response to evaluate the lipid digestion behavior by means of single-response

modeling (Section 2.5.2). A second strategy was employed to obtain mechanistic insight in lipid digestion conversions under static small intestinal *in vitro* conditions. For this purpose, we utilized the advanced statistical technique multi-response modeling (Section 2.5.3).

Single-response kinetic modeling to describe triolein cleavage

As explained in the previous section, quantified lipolysis species showed different behaviors depending on the chemical nature of the interface. Next to this, we employed single-response modeling to quantitatively evaluate these differences in the lipid digestion kinetics as affected by the emulsion interfacial composition (Figure 4). The selected response was the% of digested TAG during *in vitro* small intestinal digestion because TAGs are the main substrate for lipases. For the single-response modeling, three parameters were estimated using a fractional conversion model: (*i*) C_0 (%) represents the estimated initial value of the response, (*ii*) k (min^{-1}) is the reaction rate constant which indicates the rate at which (*iii*) C_f (%) or the plateau value is reached.

In case of C_0, it presented different values depending on the chemical nature of the emulsifiers (Table 1). The emulsifier type influenced emulsion stability and competitive adsorption between gastric lipase and the emulsifier. In brief, high extents of digested TAGs were achieved by biopolymer-stabilized emulsions (SPI and CP, 52-55%), relatively high by the LEC-stabilized emulsion (~40%), and low by NaTDC and TW80-based emulsions (3-9%). Regarding reactions rate constants k, the lowest magnitude was reached by the NaTDC-based emulsion. As explained in section 3.1, this emulsion presented a large particle size during the first part of *in vitro* small intestinal digestion which reduced the hydrolysis rate of TAG molecules. For the other emulsions, differences in k values can be explained by emulsions microstructure and particle size at the end of the gastric phase because TAGs were (almost) completely digested within the first 15 min of intestinal digestion. After 120 min of gastric digestion, TW80 and LEC-stabilized emulsions

showed the most stable d(4,3) values (0.8 and 5 μm, respectively). Conversely, SPI and CP-stabilized emulsions presented larger d(4,3) values (12 and 18 μm, respectively). This significantly impacted the magnitudes of *k*: higher rate constants reached by TW80 and LEC-stabilized emulsions (0.69 and 0.49 min^{-1}, respectively) compared to lower values reached by SPI and CP-stabilized emulsions (0.21 and 0.23 min^{-1}, respectively). The negative correlation between *k* values and initial particles size values at the beginning of small intestinal phase is shown in Figure 4B. Therefore, the stability status of the emulsion, specifically oil droplet size, at the beginning of small intestinal digestion affected the kinetics of small intestinal lipolysis during the first minutes of digestion. Bile salts apparently displaced these molecular-based interfacial layers rather easily which is possibly an evolutionary characteristic developed by mammals to fully digest lipids [50]. Consequently, competitive adsorption between emulsifiers at the interface and bile salts may have not played a major role. A similar correlation between particle size and lipid digestion extent has been reported before [13]. However, particle size has a major impact on the rate and not on the extent of lipolysis. Moreover, these authors quantified lipid digestion via titration (FFA release) and did not model the data. Regarding the extent of TAG digestion, C_f, all emulsions reached (almost) complete TAG digestion at a certain point during the small intestinal phase (Figure 4A).

In addition, the different gastric lipolysis extents did not significantly impact the lipolysis kinetics in the small intestinal phase because even a limited gastric lipolysis extent in the gastric phase resulted in fast kinetics in the small intestinal phase, e.g. TW80-based emulsion. Couëdelo et al. also found a low *in vitro* lipid digestibility in the gastric phase for a TW80 emulsion but this resulted in a lower extent of lipid hydrolysis in the following small intestinal phase compared to other emulsifiers with higher gastric lipolysis level [16]. Differences between this study and ours can be explained by different experimental conditions (e.g. emulsion preparation and/or *in vitro*

digestion parameters). In addition, the latter authors did not report microstructure evaluation nor particle size measurements during digestion which could have been useful to explain the lipid digestion behavior in the small intestinal phase. Other researchers found that only a small amount of hydrolyzed lipids is necessary to activate the pancreatic lipase complex [51]. Therefore, even a low extent of gastric lipolysis extent could be enough to trigger the lipid hydrolysis process in the small intestinal compartment. Verkempinck et al. evaluated the kinetics of lipid digestion after digesting o/w emulsions stabilized by TW80 and CP, using the INFOGEST protocol and quantifying the lipolysis products by HPLC-ELSD [43]. If we compare the extents of digested TAG in our study for TW80- and CP-based emulsions (~100%, Figure 4A) with the ones of Verkempinck et al., lower extents were found in their study: 83 and 32% for TW80 and CP, respectively. Considering the similar stability behaviors in both studies for these emulsions, the hydrolysis of triolein was probably boosted by the synergistic activity of gastric and pancreatic lipases.

Multi-response kinetic modeling for the quantitative representation of overall gastrointestinal lipolysis

As explained in Section 3.2, several lipolysis products were quantified during *in vitro* small intestinal digestion. These lipolysis products are part of a common set of (bio)chemical reactions. We aimed to elucidate these reactions via multi-response modeling. For this purpose, a reaction scheme was proposed based on previous studies on lipid digestion, lipases stereospecificity and the data generated in this study. In our previous study, we also proposed a reaction scheme describing the lipolysis phenomena under *in vitro* small intestinal conditions [23]. However, in the current study, we have included a gastric pre-lipolysis step and the quantification of more intermediate lipolysis products, which allows the construction of a more detailed reaction scheme.

443 This reaction scheme is then transformed into differential equations which solution allows the
444 estimation of kinetic parameters (reaction rate constants). The kinetic parameters hereby estimated
445 will reflect the action of several lipolytic enzymes (gastric and diverse pancreatic lipases) acting
446 simultaneously and in synergy on the same substrate and in the same reaction mixture. Afterwards,
447 the multi-response model is evaluated based on the following criteria: model convergence,
448 adjusted determination coefficient (R^2_{adj}) calculated from the experimental and predicted values
449 (parity plots), residual plots and errors of the parameter estimates. If one of these criteria is not
450 met, a new reaction scheme is proposed (iterative process).

451 After modeling the five data sets using a iterative process, the model best representing lipid
452 digestion reactions and fulfilling the previously stated criteria could only be obtained for the
453 NaTDC-based emulsion (Figure 5). Unfortunately, for all other data sets, the model derived from
454 the scheme presented in Figure 5 did not converge as well as all other logic reaction schemes tested
455 during the iterative process (data not shown). We hypothesize that the lack of convergence was
456 due to the drastic decrease in triolein concentration in a very short timeframe (Figure 3A). This
457 fast decrease was covered by only 1 or 2 experimental points which does not allow a good
458 parameter estimation. By contrast, a more progressive decrease in triolein was detected for the
459 NaTDC-based emulsion, resulting in model convergence and a better parameter estimation. A
460 representation of the multi-response model describing the lipid digestion phenomena under *in vitro*
461 small intestinal conditions is depicted in Figure 6. Predictive curves are represented as solid lines
462 and almost all of them are very close to the experimental values. The response *sn*-1,3-diolein was
463 not fitted because its concentration was very low. Regarding the modeling performance, the R^2_{adj}
464 for all responses was excellent (0.90-0.99), except for the relatively good value of *sn*-1,2/2,3-
465 diolein (0.44) which is linked to the low concentrations of this analyte during digestion. Moreover,

the residual plot shown in Figure 6G indicates that all residuals remained between the limits (represented as dotted lines).

Table 2 provides an overview of the estimated rate constants related to the six (bio)chemical reactions in the final reaction scheme (Figure 5). Enzymatic reactions involving k_1, k_3 and k_6 represent the cleavage of the *sn*-1/3 positions of the glycerol moiety. More specifically, parameters k_3 and k_6 presented the highest magnitude of all reactions. This finding is logic since pancreatic lipase was the most active enzyme, and this lipase is specific towards the extreme positions [45]. In case of k_2, the related reaction indicates the cleavage of either *sn*-1 or 3, and the *sn*-2 position. As expected, this reaction rate constant was very low since it involves the *sn*-2 position hydrolysis. We hypothesize that gastric lipase was responsible for this middle position cleavage. Gastric lipase remains active during the small intestinal phase and contributes to around 7.5% of lipid digestion in this compartment [46]. In our previous study, we detected the gastric lipase capacity to catalyze the breakage of the ester bond at the *sn*-2 position [24]. Other authors have also suggested the affinity of gastric lipase towards this position [48,52]. Finally, k_4 and k_5 kinetic parameters involved isomerization reactions. This type of reaction was proposed in the scheme because migration of fatty acids located at the *sn*-2 towards the *sn*-1/3 positions has been reported before [53]. Compared to the enzymatic conversions, isomerization reactions are rather slow but still contribute to the lipid digestion process.

In brief, this research aimed to evaluate the effect of different emulsion interfacial composition on the lipid digestion kinetics and to elucidate the lipolysis mechanism under *in vitro* small intestinal conditions including a gastric pre-lipolysis step using advanced modeling techniques. The interfacial composition can modulate lipolysis kinetics by influencing the emulsion stability and/or competitive adsorption for the interface between digestive elements and emulsifiers. In case of the

model emulsions employed in this study, the rather simple interfacial layer(s) seemed to allow very fast kinetics of lipid digestion in the small intestinal phase. Hence, the main factor impacting the lipolysis kinetics, especially the reaction rate constant during the first minutes of small intestinal digestion, was the stability of emulsions resulting from the gastric digestion step. This was indicated by the negative correlation between the estimated reaction rate constant by single-response modeling and the average droplet size. It was aimed to elucidate the lipolysis molecular mechanism using multi-response modeling. Enzymatic and chemical conversions were included in the final reaction scheme. The enzymatic cleavage of the *sn*-1/3 positions were the fastest conversions followed by isomerization reactions and *sn*-2 ester bond hydrolysis. To sum up, molecular-based interfacial layers seem not to represent a barrier for lipid hydrolysis in the small intestinal phase. However, the stability changes during the gastric phase resulting from using diverse emulsifiers affected the kinetics in the small intestinal phase. Further detailed studies including the use of interfacial multi-layers or more complex interfaces are needed to understand how lipolysis kinetics can be modulated in the digestive compartments. Additionally, further characterization of interfaces (e.g. interfacial tension) during *in vitro* digestion would give more insights on the competitive adsorption phenomenon between emulsifiers and bile salts and lipases.

Acknowledgement

We would like to thank Nordmark (Uetersen, Germany) for providing us with the pancreatic extract.

Declaration of interests

The authors of this work declare no conflict of interests.

Supporting information

Microstructural changes of the five emulsions subjected to *in vitro* gastrointestinal digestion

References

1. Bénarouche, A., Point, V., Carrière, F. & Cavalier, J. F. Using the reversible inhibition of gastric lipase by Orlistat for investigating simultaneously lipase adsorption and substrate hydrolysis at the lipid-water interface. *Biochimie* **101**, 221–231 (2014).

2. Muth, M., Rothkötter, S., Paprosch, S., Schmid, R. P. & Schnitzlein, K. Competition of Thermomyces lanuginosus lipase with its hydrolysis products at the oil–water interface. *Colloids Surfaces B Biointerfaces* **149**, 280–287 (2017).

3. Reis, P. *et al.* Lipase reaction at interfaces as self-limiting processes. *Comptes Rendus Chim.* **12**, 163–170 (2009).

4. Sarkar, A., Ye, A. & Singh, H. On the role of bile salts in the digestion of emulsified lipids. *Food Hydrocoll.* **60**, 77–84 (2016).

5. Scheuble, N., Lussi, M., Geue, T., Carrière, F. & Fischer, P. Blocking Gastric Lipase Adsorption and Displacement Processes with Viscoelastic Biopolymer Adsorption Layers. *Biomacromolecules* **17**, 3328–3337 (2016).

6. Verkempinck, S. H. E. *et al.* Emulsion stability during gastrointestinal conditions effects lipid digestion kinetics. *Food Chem.* **246**, 179–191 (2018).

7. Wang, X., Lin, Q., Ye, A., Han, J. & Singh, H. Flocculation of oil-in-water emulsions stabilised by milk protein ingredients under gastric conditions: Impact on in vitro intestinal lipid digestion. *Food Hydrocoll.* **88**, 272–282 (2019).

8. Liu, L., Pan, Y., Zhang, X., Zhang, Y. & Li, X. Effect of Particle Size and Interface Composition on the Lipid Digestion of Droplets Covered with Membrane Phospholipids.

J. Agric. Food Chem. **13**, 29 (2020).

9. Liang, L., Zhang, X., Wang, X., Jin, Q. & McClements, D. J. Influence of dairy emulsifier type and lipid droplet size on gastrointestinal fate of model emulsions: In vitro digestion study. *J. Agric. Food Chem.* **66**, 9761–9769 (2018).

10. Ye, A., Wang, X., Lin, Q., Han, J. & Singh, H. Dynamic gastric stability and in vitro lipid digestion of whey-protein-stabilised emulsions: Effect of heat treatment. *Food Chem.* **318**, 126463 (2020).

11. Maljaars, P., Peters, H., Mela, D. & Masclee, A. Ileal brake: A sensible food target for appetite control. A review. *Physiol. Behav.* **95**, 271–281 (2008).

12. Katouzian, I., Faridi Esfanjani, A., Jafari, S. M. & Akhavan, S. Formulation and application of a new generation of lipid nano-carriers for the food bioactive ingredients. *Trends Food Sci. Technol.* **68**, 14–25 (2017).

13. Tan, Y., Zhang, Z., Muriel Mundo, J. & McClements, D. J. Factors impacting lipid digestion and nutraceutical bioaccessibility assessed by standardized gastrointestinal model (INFOGEST): Emulsifier type. *Food Res. Int.* **137**, 109739 (2020).

14. Park, S., Mun, S. & Kim, Y. R. Emulsifier Dependent in vitro Digestion and Bioaccessibility of β-Carotene Loaded in Oil-in-Water Emulsions. *Food Biophys.* **13**, 147–154 (2018).

15. Malaki Nik, A., Wright, A. J. & Corredig, M. Impact of interfacial composition on emulsion digestion and rate of lipid hydrolysis using different in vitro digestion models. *Colloids Surfaces B Biointerfaces* **83**, 321–330 (2011).

16. Couëdelo, L. *et al.* Impact of various emulsifiers on ALA bioavailability and chylomicron synthesis through changes in gastrointestinal lipolysis. *Food Funct.* **6**, 1726–1735 (2015).

17. Chang, Y. & McClements, D. J. Influence of emulsifier type on the in vitro digestion of fish oil-in-water emulsions in the presence of an anionic marine polysaccharide (fucoidan): Caseinate, whey protein, lecithin, or Tween 80. *Food Hydrocoll.* **61**, 92–101 (2016).

18. Bellesi, F. A., Martinez, M. J., Pizones Ruiz-Henestrosa, V. M. & Pilosof, A. M. R. Comparative behavior of protein or polysaccharide stabilized emulsion under in vitro gastrointestinal conditions. *Food Hydrocoll.* **52**, 47–56 (2016).

19. Gargouri, Y. *et al.* Importance of human gastric lipase for intestinal lipolysis: an in vitro study. *Biochim. Biophys. Acta (BBA)/Lipids Lipid Metab.* **879**, 419–423 (1986).

20. Sassene, P. J. *et al.* Comparison of lipases for in vitro models of gastric digestion: lipolysis using two infant formulas as model substrates. *Food Funct.* **7**, 3989–3998 (2016).

21. van Boekel, M. A. J. S. Kinetic Modeling of Food Quality: A Critical Review. *Compr. Rev. Food Sci. Food Saf.* **7**, 144–158 (2008).

22. Giang, T. M. *et al.* Dynamic modeling of in vitro lipid digestion: Individual fatty acid release and bioaccessibility kinetics. *Food Chem.* **194**, 1180–1188 (2016).

23. Verkempinck, S. H. E., Salvia-Trujillo, L., Infantes Garcia, M. R., Hendrickx, M. E. & Grauwet, T. From single to multiresponse modelling of food digestion kinetics: The case of lipid digestion. *J. Food Eng.* **260**, 40–49 (2019).

24. Infantes-Garcia, M. R. *et al.* Enzymatic and chemical conversions taking place during in

vitro gastric lipid digestion: The effect of emulsion droplet size behavior. *Food Chem.* **326**, 126895 (2020).

25. Li, Y. & Mcclements, D. J. New mathematical model for interpreting ph-stat digestion profiles: Impact of lipid droplet characteristics on in vitro digestibility. *J. Agric. Food Chem.* **58**, 8085–8092 (2010).

26. Tiruppathi, C. & Balasubramanian, K. A. Purification and properties of an acid lipase from human gastric juice. *Biochim. Biophys. Acta (BBA)/Lipids Lipid Metab.* **712**, 692–697 (1982).

27. Constantin, M. J., Pasero, L. & Desnuelle, P. Quelques remarques complémentaires sur l'hydrolyse des triglycerides par la lipase pancréatique. *BBA - Biochim. Biophys. Acta* **43**, 103–109 (1960).

28. Mitchell, D. A., Rodriguez, J. A., Carrière, F., Baratti, J. & Krieger, N. An analytical method for determining relative specificities for sequential reactions catalyzed by the same enzyme: Application to the hydrolysis of triacylglycerols by lipases. *J. Biotechnol.* **133**, 343–350 (2008).

29. Lawrence, M. J. & Rees, G. D. Microemulsion-based media as novel drug delivery systems. *Adv. Drug Deliv. Rev.* **64**, 175–193 (2012).

30. Tang, C.-H. Emulsifying properties of soy proteins: A critical review with emphasis on the role of conformational flexibility. *Crit. Rev. Food Sci. Nutr.* **57**, 2636–2679 (2017).

31. Verkempinck, S. H. E. *et al.* Emulsion stabilizing properties of citrus pectin and its interactions with conventional emulsifiers in oil-in-water emulsions. *Food Hydrocoll.* **85**,

144–157 (2018).

32. Karupaiah, T. & Sundram, K. Effects of stereospecific positioning of fatty acids in triacylglycerol structures in native and randomized fats: a review of their nutritional implications. *Nutr. Metab. (Lond).* **4**, 16 (2007).

33. Infantes-Garcia, M. R., Verkempinck, S. H. E., Gonzalez-Fuentes, P. G., Hendrickx, M. E. & Grauwet, T. Lipolysis products formation during in vitro gastric digestion is affected by the emulsion interfacial composition. *Food Hydrocoll.* **110**, 106163 (2021).

34. Brodkorb, A. *et al.* INFOGEST static in vitro simulation of gastrointestinal food digestion. *Nat. Protoc.* **14**, 991–1014 (2019).

35. Salvia-Trujillo, L. *et al.* Lipid digestion, micelle formation and carotenoid bioaccessibility kinetics: Influence of emulsion droplet size. *Food Chem.* **229**, 653–662 (2017).

36. Macierzanka, A., Torcello-Gómez, A., Jungnickel, C. & Maldonado-Valderrama, J. Bile salts in digestion and transport of lipids. *Adv. Colloid Interface Sci.* **274**, 102045 (2019).

37. Maldonado-Valderrama, J., Wilde, P., Macierzanka, A. & Mackie, A. The role of bile salts in digestion. *Adv. Colloid Interface Sci.* **165**, 36–46 (2011).

38. Lin, X., Wang, Q., Li, W. & Wright, A. J. Emulsification of algal oil with soy lecithin improved DHA bioaccessibility but did not change overall in vitro digestibility. *Food Funct.* **5**, 2913–2921 (2014).

39. Golding, M. *et al.* Impact of gastric structuring on the lipolysis of emulsified lipids. *Soft Matter* **7**, 3513 (2011).

40. Chove, B. E., Grandison, A. S. & Lewis, M. J. Emulsifying properties of soy protein

isolate fractions obtained by isoelectric precipitation. *J. Sci. Food Agric.* **81**, 759–763 (2001).

41. Singh, H. & Ye, A. Structural and biochemical factors affecting the digestion of protein-stabilized emulsions. *Curr. Opin. Colloid Interface Sci.* **18**, 360–370 (2013).

42. Nishinari, K., Fang, Y., Guo, S. & Phillips, G. O. Soy proteins: A review on composition, aggregation and emulsification. *Food Hydrocoll.* **39**, 301–318 (2014).

43. Verkempinck, S. H. E. *et al.* Pectin influences the kinetics of in vitro lipid digestion in oil-in-water emulsions. *Food Chem.* **262**, 150–161 (2018).

44. Du Le, H., Loveday, S. M., Nowak, E., Niu, Z. & Singh, H. Pectin emulsions for colon-targeted release of propionic acid. *Food Hydrocoll.* **103**, 105623 (2020).

45. Carrière, F. *et al.* In vivo and in vitro studies on the stereoselective hydrolysis of tri- and diglycerides by gastric and pancreatic lipases. *Bioorg. Med. Chem.* **5**, 429–435 (1997).

46. Carrière, F., Barrowman, J., Verger, R. & Laugier, R. Secretion and contribution to lipolysis of gastric and pancreatic lipases during a test meal in humans. *Gastroenterology* **105**, 876–888 (1993).

47. Rodriguez, J. A. *et al.* Novel chromatographic resolution of chiral diacylglycerols and analysis of the stereoselective hydrolysis of triacylglycerols by lipases. *Anal. Biochem.* **375**, 196–208 (2008).

48. Rogalska, E., Ransac, S. & Vergers, R. Stereoselectivity of Lipases II. Stereoselective hydrolysis of triglycerides by gastric and pancreatic lipases. *J. Biol. Chem.* **265**, 20271–20276 (1990).

638 49. Scheuble, N. *et al.* Microfluidic Technique for the Simultaneous Quantification of
639 Emulsion Instabilities and Lipid Digestion Kinetics. *Anal. Chem.* **89**, 9116–9123 (2017).

640 50. Bai, L. *et al.* Oil-in-water Pickering emulsions via microfluidization with cellulose
641 nanocrystals: 2. In vitro lipid digestion. *Food Hydrocoll.* **96**, 709–716 (2019).

642 51. Borel, P. *et al.* Hydrolysis of emulsions with different triglycerides and droplet sizes by
643 gastric lipase in vitro. Effect on pancreatic lipase activity. *J. Nutr. Biochem.* **5**, 124–133
644 (1994).

645 52. Rodriguez, J. A. *et al.* In vitro stereoselective hydrolysis of diacylglycerols by hormone-
646 sensitive lipase. *Biochim. Biophys. Acta - Mol. Cell Biol. Lipids* **1801**, 77–83 (2010).

647 53. Serdarevich, B. Glyceride isomerizations in lipid chemistry. *J. Am. Oil Chem. Soc.* **44**,
648 381–393 (1967).

649 # Funding

650 M.R. Infantes-Garcia is a Doctoral Researcher funded by the Research Foundation Flanders (FWO
651 - Grant No. 1S03318N). S.H.E. Verkempinck is a Postdoctoral Researcher funded by the Research
652 Foundation Flanders (FWO - Grant No. 1222420N). The authors also acknowledge the financial
653 support of the Internal Funds KU Leuven

Figure Captions

Figure. 1. Evolution of the ζ-potential of sodium taurodeoxycholate (NaTDC), lecithin (LEC), soy protein isolate (SPI), citrus pectin (CP) and tween 80 (TW80) based emulsions during in vitro gastric and small intestinal digestion. Different lower case letters indicate significant differences ($P < 0.05$) between different digestion times from the same emulsion.

Figure 2. Evolution of the particle size distribution (PSD) and average volume-based particle size d(4,3) of sodium taurodeoxycholate (NaTDC), lecithin (LEC), soy protein isolate (SPI), citrus pectin (CP) and tween 80 (TW80) based emulsions during *in vitro* gastric (0-120 min) and small intestinal digestion (120-240 min).

Figure 3. Time dependency of (A) triolein and (B, C, D, E, F, G) multiple lipolysis products during in vitro small intestinal digestion as affected by the interfacial composition of oil-in-water emulsions. Glycerol was calculated based on the quantified lipolysis products. Symbols represent the experimental values of the analyte concentration for the (▼) sodium taurodeoxycholate (NaTDC), (○) lecithin (LEC), (◆) soy protein isolate (SPI), (△) citrus pectin (CP), and (□) tween 80 (TW80) based emulsion.

Figure 4. Time dependency of (A) digested triolein during *in vitro* small intestinal digestion as affected by the interfacial composition of oil-in-water emulsions. (B) Correlation between the average particle size d(4,3) value at the beginning of the intestinal phase and the reaction rate constant k (min^{-1}) of digested triolein for emulsions formulated with different emulsifiers. Symbols in graphs A represent the experimental values of the analyte concentration for the (▼) sodium taurodeoxycholate (NaTDC), (○) lecithin (LEC), (◆) soy protein isolate (SPI), (△) citrus pectin (CP), and (□) tween 80 (TW80) based emulsion. Dot-dashed, dashed, solid, dotted and double-

dot-dashed lines in graph A represent the predicted values of the corresponding fractional conversion model for digested triolein of the NaTDC-, LEC-, SPI-, CP- and TW80-based emulsion, respectively. In graph B, from left to right, data points correspond to the TW80-, LEC-, SPI-, PEC- and NaTDC-based emulsions.

Figure 5. (A) Final reaction scheme postulated to describe the lipolysis mechanism under *in vitro* small intestinal conditions. (B) Differential equations derived from the final reaction scheme.

Figure 6. (A, B, C, D, E, F) Representation of the multi-response modeling describing the lipolysis products evolution during in vitro gastric digestion for the (▼) sodium taurodeoxycholate (NaTDC) based emulsion. Solid lines are the predicted curves for each analyte. (G) Residual plot derived from the multi-response model. Roman numbers indicate the standardized residual set of points for (I) triolein; (II) sn-1,2/2,3-diolein; (III) sn-2-monoolein; (IV) sn-1/3-monoolein; (V) oleic acid and (VI) glycerol.

Table 1. Single-response Model Parameter Estimates of the Percentage of Digested Triolein during *In Vitro* Small Intestinal Digestion of the Sodium Taurodeoxycholate (NaTDC), Lecithin (LEC), Soy Protein Isolate (SPI), Citrus Pectin (CP), and Tween 80 (TW80) Based Emulsions. Different Lower Case Letters Indicate Significant Differences among each Parameter Estimate according to their Confidence Intervals (95%). The Parameter C_0 is the Estimated Initial Concentration, k is the Estimated Lipolysis Rate Constant, and C_f is the Estimated Final Extent of TAG Hydrolysis.

	% Digested triolein		
	C_0 **(%)**	k **(min^{-1})**	C_f **(%)**
NaTDC	8.9 ± 6.8[a]	0.05 ± 0.01 [a]	101.4 ± 5.0 [a]
LEC	40.3 ± 0.2 [b]	0.49 ± 0.01 [b]	100.1 ± 0.0 [a]
SPI	55.2 ± 2.7 [c]	0.21 ± 0.04 [c]	96.4 ± 1.2 [a]
CP	52.4 ± 1.3 [c]	0.23 ± 0.02 [c]	98.8 ± 0.6 [a]
TW80	2.66 ± 0.0 [a]	0.69 ± 0.00 [d]	100.0 ± 0.0 [a]

Table 2. Estimated Kinetic Parameters Determined after the Multi-Response Modeling of the *In Vitro* Small Intestinal Digestion of the NaTDC-Based Emulsion. The Parameter k_{number} (min^{-1}) Represents the Reaction Rate Constants for a certain (Bio)Chemical Conversion. Different Lower Case Letters Indicate Significant Differences among each Parameter Estimate According to their Confidence Intervals (95%).

$\boldsymbol{k_1}$	0.0027 ± 0.0007^{a}
$\boldsymbol{k_2}$	0.0050 ± 0.0016^{b}
$\boldsymbol{k_3}$	0.0403 ± 0.0026^{c}
$\boldsymbol{k_4}$	0.0060 ± 0.0008^{b}
$\boldsymbol{k_5}$	0.0060 ± 0.0008^{b}
$\boldsymbol{k_6}$	0.0172 ± 0.0018^{d}

Figure 1

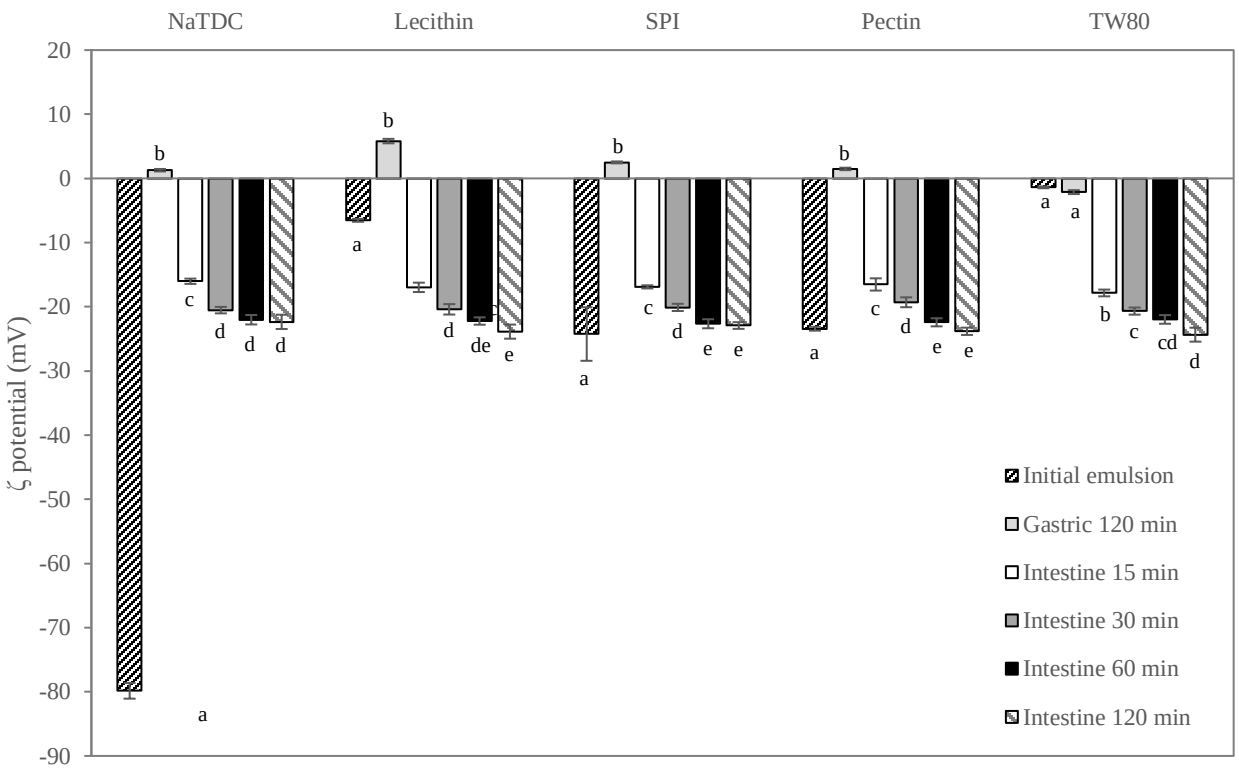
NaTDC
Lecithin
SPI
Pectin
TW80
ζ potential (mV)
20
10
0
-10
-20
-30
-40
-50
-60
-70
-80
-90
Initial emulsion
Gastric 120 min
Intestine 15 min
Intestine 30 min
Intestine 60 min
Intestine 120 min

Figure 2

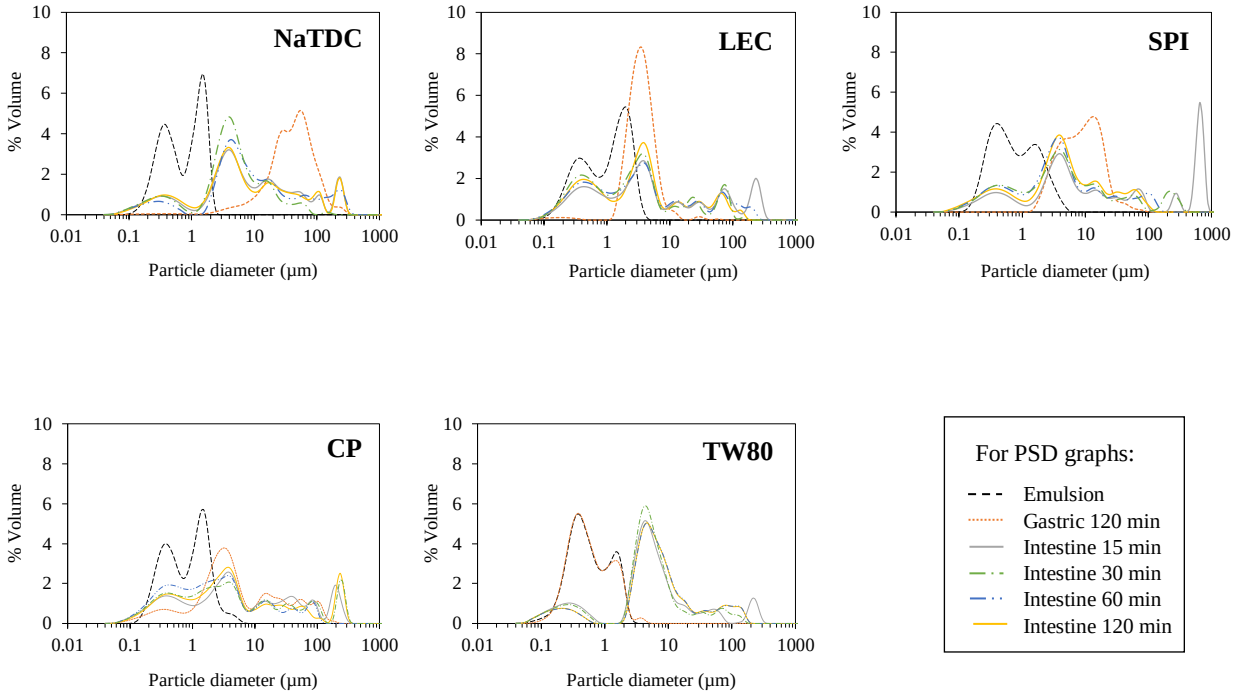
NaTDC
LEC
SPI
CP
TW80
% Volume
Particle diameter (µm)
For PSD graphs:
Emulsion
Gastric 120 min
Intestine 15 min
Intestine 30 min
Intestine 60 min
Intestine 120 min

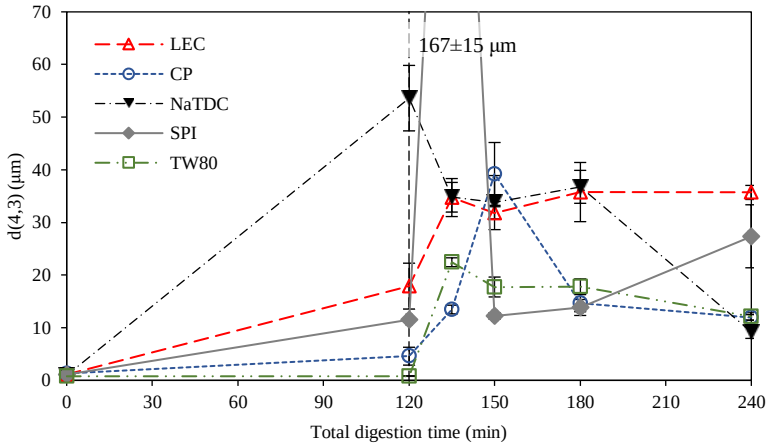
LEC
CP
NaTDC
SPI
TW80
167±15 µm
d(4,3) (µm)
Total digestion time (min)

Figure 3

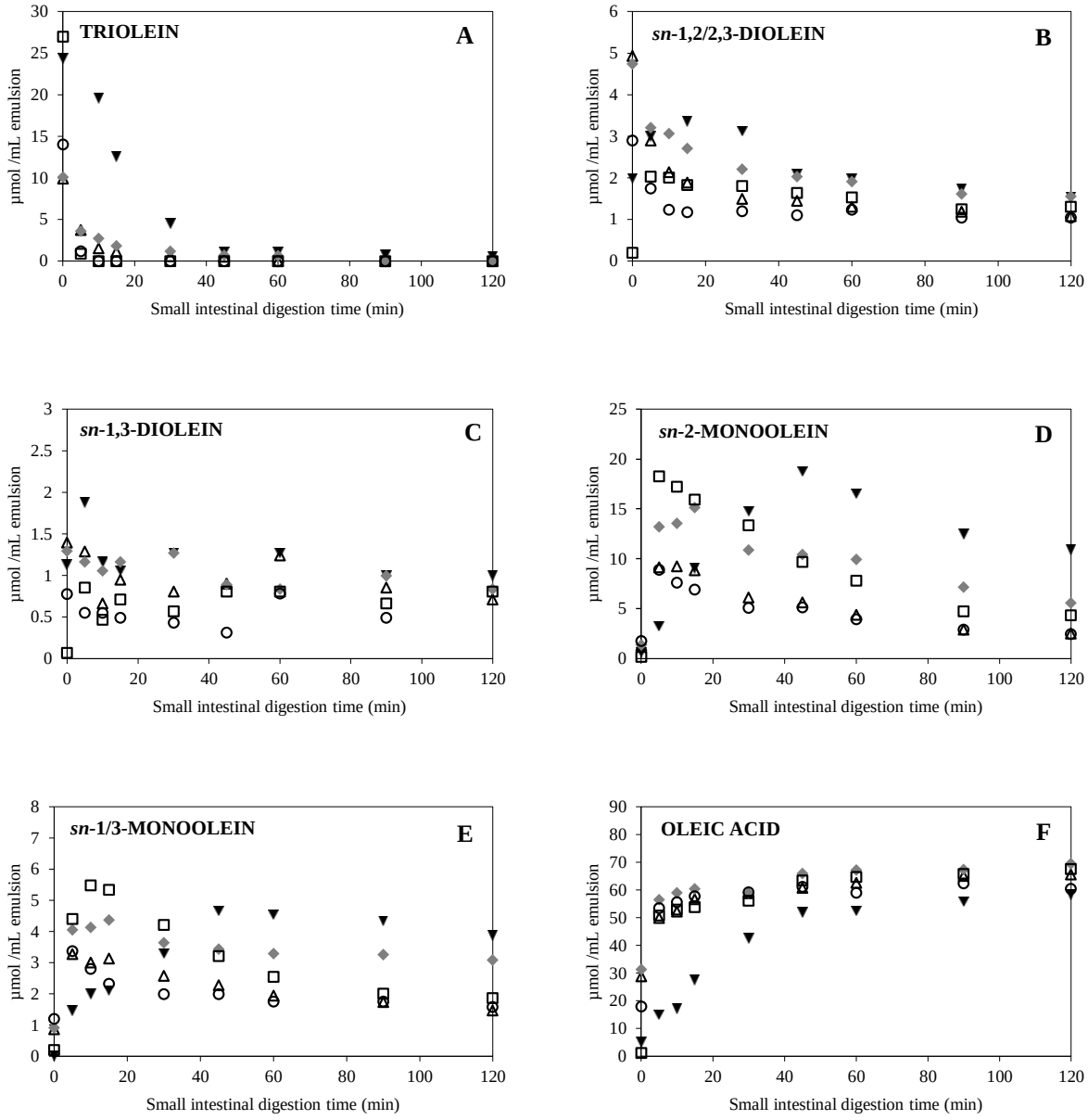
TRIOLEIN
A
µmol /mL emulsion
Small intestinal digestion time (min)
sn-1,2/2,3-DIOLEIN
B
µmol /mL emulsion
Small intestinal digestion time (min)
sn-1,3-DIOLEIN
C
µmol /mL emulsion
Small intestinal digestion time (min)
sn-2-MONOOLEIN
D
µmol /mL emulsion
Small intestinal digestion time (min)
sn-1/3-MONOOLEIN
E
µmol /mL emulsion
Small intestinal digestion time (min)
OLEIC ACID
F
µmol /mL emulsion
Small intestinal digestion time (min)

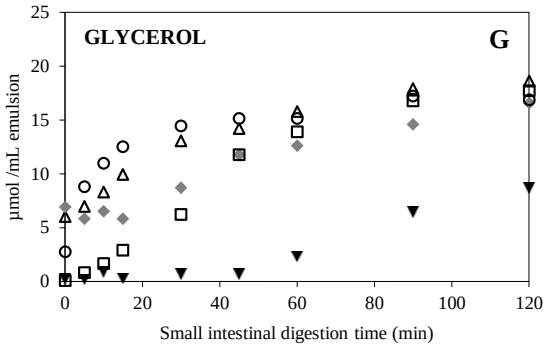
GLYCEROL
G
µmol /mL emulsion
Small intestinal digestion time (min)
0
5
10
15
20
25
0
20
40
60
80
100
120

Figure 4

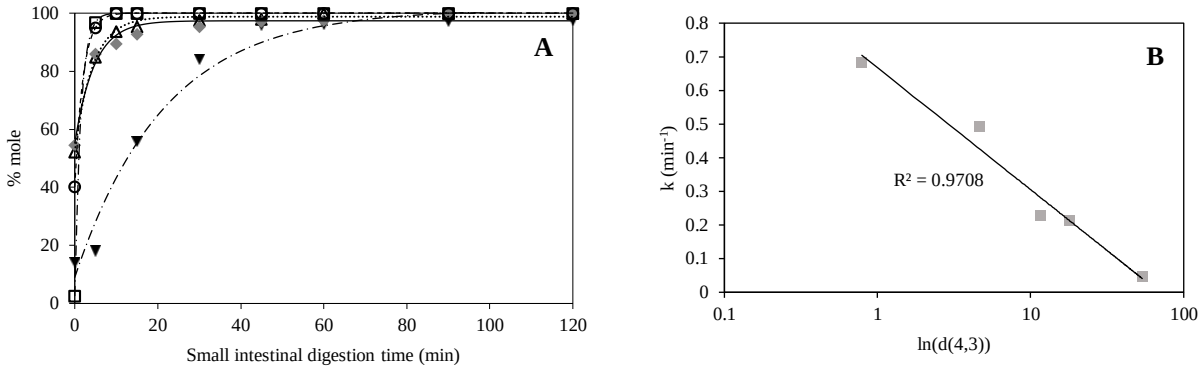
A
% mole
Small intestinal digestion time (min)
0
20
40
60
80
100
120
B
k (min-1)
R² = 0.9708
ln(d(4,3))
0.1
1
10
100

Figure 5

A

$$\mathrm{TAG} + \mathrm{H_2O} \xrightarrow{k_1} sn\text{-}1,2/2,3\text{-DAG} + \mathrm{FFA}$$

$$\mathrm{TAG} + 2\mathrm{H_2O} \xrightarrow{k_2} sn\text{-}1/3\text{-MAG} + 2\mathrm{FFA}$$

$$\mathrm{TAG} + 2\mathrm{H_2O} \xrightarrow{k_3} sn\text{-}2\text{-MAG} + 2\mathrm{FFA}$$

$$sn\text{-}1,2/2,3\text{-DAG} \xrightarrow{k_4} sn\text{-}1,3\text{-DAG}$$

$$sn\text{-}2\text{-MAG} \xrightarrow{k_5} sn\text{-}1/3\text{-MAG}$$

$$sn\text{-}1/3\text{-MAG} + \mathrm{H_2O} \xrightarrow{k_6} \mathrm{FFA} + \mathrm{GLY}$$

B

$$\frac{d(\mathrm{TAG})}{dt} = -(k_1+k_2+k_3)(\mathrm{TAG})$$

$$\frac{d(sn\text{-}1,2/2,3\text{-DAG})}{dt} = k_1(\mathrm{TAG}) - k_4(sn\text{-}1,2/2,3\text{-DAG})$$

$$\frac{d(sn\text{-}1,3\text{-DAG})}{dt} = k_4(sn\text{-}1,2/2,3\text{-DAG})$$

$$\frac{d(sn\text{-}2\text{-MAG})}{dt} = k_3(\mathrm{TAG}) - k_5(sn\text{-}2\text{-MAG})$$

$$\frac{d(sn\text{-}1/3\text{-MAG})}{dt} = k_2(\mathrm{TAG}) + k_5(sn\text{-}2\text{-MAG}) - k_6(sn\text{-}1/3\text{-MAG})$$

$$\frac{d(\mathrm{FFA})}{dt} = (k_1+2k_2+2k_3)(\mathrm{TAG}) + k_6(sn\text{-}1/3\text{-MAG})$$

$$\frac{d(\mathrm{GLY})}{dt} = k_6(sn\text{-}1/3\text{-MAG})$$

Figure 6

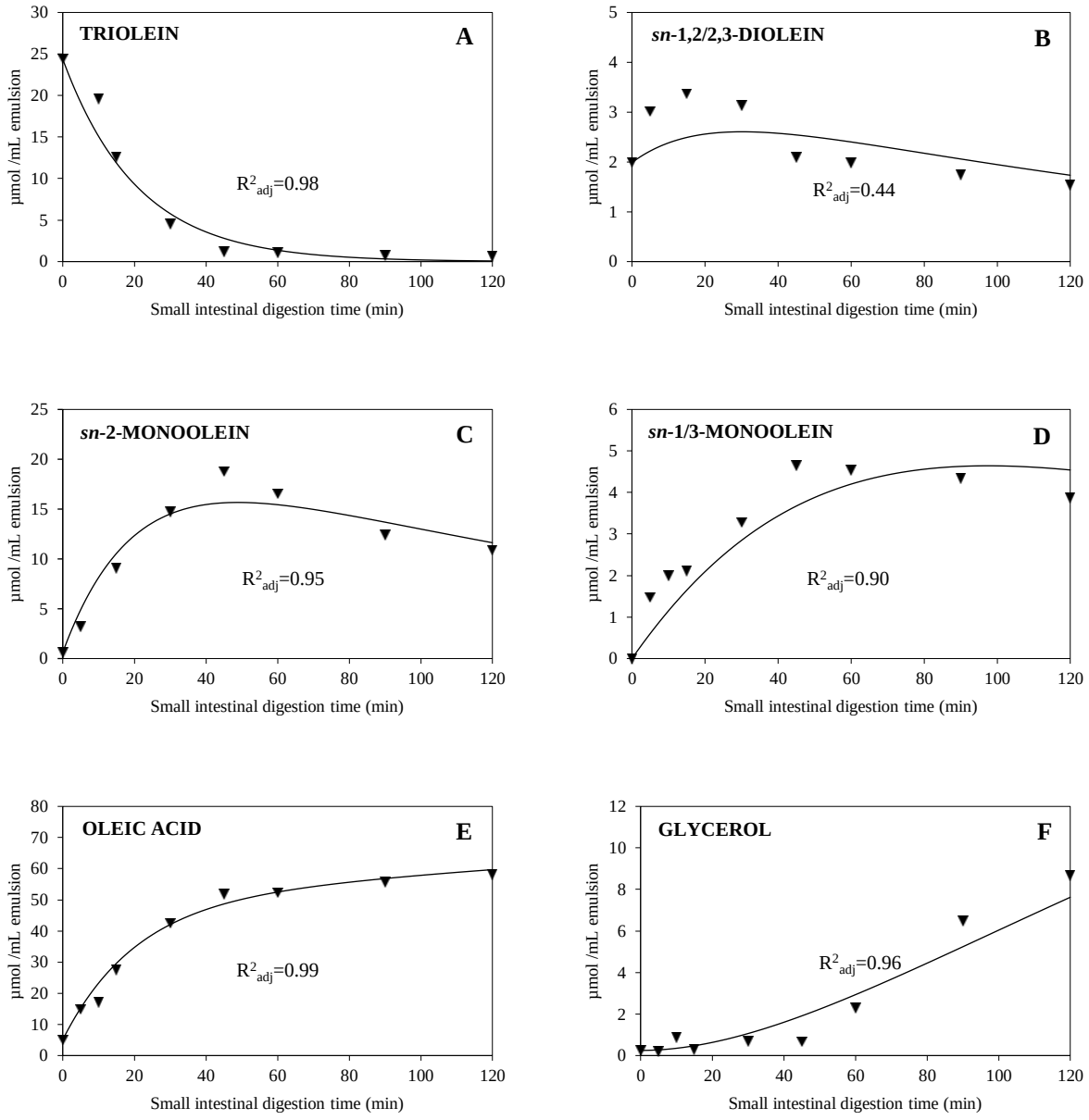
TRIOLEIN
A
R2adj=0.98
sn-1,2/2,3-DIOLEIN
B
R2adj=0.44
sn-2-MONOOLEIN
C
R2adj=0.95
sn-1/3-MONOOLEIN
D
R2adj=0.90
OLEIC ACID
E
R2adj=0.99
GLYCEROL
F
R2adj=0.96
µmol /mL emulsion
Small intestinal digestion time (min)

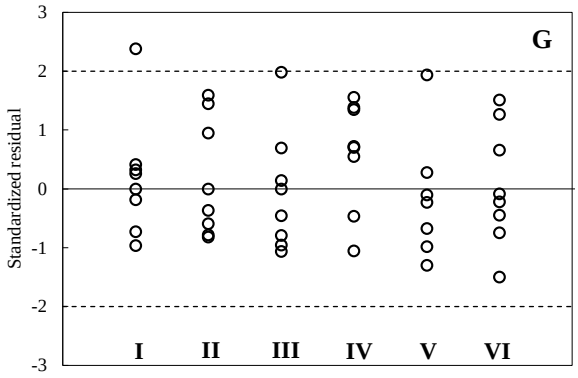
G
Standardized residual
3
2
1
0
-1
-2
-3
I
II
III
IV
V
VI

Abstract

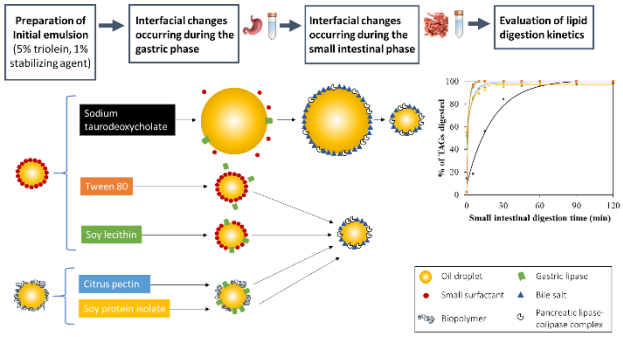
Preparation of Initial emulsion (5% triolein, 1% stabilizing agent)
Interfacial changes occurring during the gastric phase
Interfacial changes occurring during the small intestinal phase
Evaluation of lipid digestion kinetics
Sodium taurodeoxycholate
Tween 80
Soy lecithin
Citrus pectin
Soy protein isolate
% of TAGs digested
Small intestinal digestion time (min)
Oil droplet
Small surfactant
Biopolymer
Gastric lipase
Bile salt
Pancreatic lipase-colipase complex